Brief paper

Static anti-windup with shifted equilibria applied to a Segway-like vehicle☆

Philipp Braun [a],*, Abhishek Bhardwaj [a], Mirko Brentari [b], Luca Zaccarian [b,c], Matteo Saveriano [b]

[a] *School of Engineering, Australian National University, Australia*
[b] *Department of Industrial Engineering, University of Trento, Italy*
[c] *LAAS-CNRS, Université de Toulouse, Toulouse, France*

A B S T R A C T

Leveraging recent results on bounded stabilization of linear plants using shifted equilibria, we propose a novel anti-windup scheme for linear input-saturated plants with (asymmetric) saturation limits. We show that, with open-loop plants involving a continuum of equilibria, the proposed anti-windup solution provides an unbounded estimate of the basin of attraction, thereby overcoming typical limits of classical solutions. We also report on experiments performed on a segway-like vehicle, where the controller effectively displaces the segway between any two locations, due to unboundedness of the basin of attraction.

1. Introduction

Anti-windup designs augment a pre-specified controller with modifications that are only activated in the medium signal range, where saturation becomes relevant for the closed-loop response (Tarbouriech & Turner, 2009; Zaccarian & Teel, 2011). Concentrating on the medium signal behavior, rather than insisting on large signal (or even global) stability properties is somewhat necessary. Indeed, it was proven in Sontag (1984) that no linear plant can be globally exponentially stabilized with a bounded input, unless it is already open-loop exponentially stable. What is rarely exploited is the fact that for many saturated plants, the null-controllability set (i.e. the set from where there exists an input driving the response to zero) is unbounded in certain relevant directions. It is therefore relevant to seek for anti-windup solutions providing unbounded basins of attractions.

Such a feature is intrinsically absent in the classical so-called Direct-Linear Anti-windup (DLAW) paradigm, which focuses on quadratic Lyapunov functions and ellipsoidal (therefore bounded) estimates of the basin of attraction (see the works in Cao, Lin, and Ward (2002), Hu, Teel, and Zaccarian (2008), Gomes da Silva and Tarbouriech (2005) and Mulder, Kothare, and Morari (2001), just to cite a few). Several piecewise quadratic generalizations have also been proposed (Dai, Hu, Teel, & Zaccarian, 2009; Lu & Lin, 2011; Queinnec, Tarbouriech, Valmorbida, & Zaccarian, 2022), mostly to be used as a-posteriori tools for obtaining larger estimates of the basin of attraction, but for all of these cases one only gets bounded estimates comprising compact sublevel sets of radially unbounded (possibly nonquadratic) functions.

In this paper, following the paradigm of Braun, Giordano, Kellett, and Zaccarian (2021) and Mariano, Blanchini, Formentin, and Zaccarian (2020) we propose a nonlinear anti-windup certifying (possibly unbounded) estimates of the basin of attraction obtained by gradually moving toward the origin, guided by centroids of a family of ellipsoidal sets. These centroids are induced equilibria for the given plant-controller pair attained by using a portion of the control authority (always less than limits). The rest of the control authority is used to stabilize such equilibria, which are then gradually shifted to the origin via periodic or continuous updating. When the centroids are induced equilibria requiring nonzero control inputs (e.g., if the plant has a single equilibrium), our nonlinear anti-windup solution well manages asymmetric saturation levels, due to the property that the shifting mechanism allows for a virtual manipulation of the saturation limits through an appropriate translation (see also Braun et al. (2021)

* Corresponding author.
E-mail addresses: philipp.braun@anu.edu.au (P. Braun), Abhishek.Bhardwaj@anu.edu.au (A. Bhardwaj), mirko.brentari@unitn.it (M. Brentari), zaccarian@laas.fr (L. Zaccarian), matteo.saveriano@unitn.it (M. Saveriano).

and Mariano et al. (2020) for a similar result in a direct one-step saturated state feedback design context). When the centroids are induced equilibria requiring zero control inputs the shifting approach allows obtaining unbounded unions of ellipsoids and unbounded basins of attraction: a fact that we illustrate well in a segway-like application example. To deal with unbounded viable sets, we embed state-dependent activation mechanisms based on suitable safe/unsafe sets, thus requiring a measurement of the plant state. This approach has been used before when wanting to provide large regions of attraction with exponentially unstable linear plants (Barbu, Galeani, Teel, & Zaccarian, 2005; Galeani, Teel, & Zaccarian, 2007; Teel, 1999), Zaccarian and Teel (2011, §8.5). While the anti-windup action can be both activated by the occurrence of saturation or by the state being too far from the origin, the prescribed closed-loop still remains unmodified for sufficiently small closed-loop responses. Our design is based on an online solution of a convex optimization problem. As such, it shares interesting similarities with (sampled-data) model predictive control techniques for bounded stabilization of linear plants (Rawlings, Mayne, & Diehl, 2017), as well as the more specific reference (or command) governor schemes, well surveyed in the recent work (Nicotra & Garone, 2018). As compared to those works, our solution has the potential of being computationally much more attractive or requiring less memory, and implementable on low-cost hardware: a fact that we illustrate by way of experimental results on a segway-like vehicle operated by a low-cost Arduino board.

The paper is organized as follows. In Section 2 we overview the DLAW formulation. Section 3 characterizes shifted equilibria and their characterization. Section 4 presents our anti-windup solution and the main result. Section 5 discusses the above-mentioned computationally cheap implementation used in Section 6 for set-point regulation of a segway-like vehicle application.

Notation. We use $\cdot^\top$ to denote the transpose of a vector/matrix. Function $\min(\cdot)$ denotes the minimum of a row vector $a \in \mathbb{R}^m$, i.e., $\min(a) = \min\{a_i \in \mathbb{R}| i = 1, \ldots, m\} \in \mathbb{R}$, or the component-wise minimum of a matrix $A \in \mathbb{R}^{m \times 2}$, i.e., $\min(A) \in \mathbb{R}^m$. The maximum $\max(\cdot)$ is defined in the same way. For $u^-, u^+ \in \mathbb{R}^m_{\geq 0}$, $m \in \mathbb{N}$, $\mathrm{sat}_{[u^-, u^+]}(u) = \max([\min[u^+ u] - u^-])$ defines the saturation and $\mathrm{dz}_{[u^-, u^+]}(u) = u - \mathrm{sat}_{[u^-, u^+]}(u)$ denotes the deadzone. For $Z \in \mathbb{R}^{n \times n}$, $\mathrm{He}(Z) = Z + Z^\top$. For $Z \in \mathbb{R}^{n \times m}$ and $z \in \mathbb{R}^n$, $Z_{[k]}$ and z_k denote the kth row and the kth entry, respectively. A vector $v \in \mathbb{R}^n$ satisfies $v \leq \min([u^- \ u^+])$ if $v_k \leq \min([u_k^- u_k^+])$ for all $k \in \{1, \ldots, n\}$. In $\mathbb{R}^n$, we use the norms $|x| = \sqrt{x^\top x}$ and $|x|_P = \sqrt{x^\top P x}$, with $P \in \mathbb{R}^{n \times n}$ positive definite, and $|\cdot|_1$ denotes the 1-norm. The spectral norm is denoted by $\|A\| = \sqrt{\lambda_{\max}(A^\top A)}$, $A \in \mathbb{R}^{n \times m}$. Moreover, $I \in \mathbb{R}^{n \times n}$ denotes the identity matrix, $\mathbb{1}$ satisfies $\mathbb{1}_k = 1$, $k \in \{1, \ldots, n\}$, and $\mathrm{int}(\mathcal{A})$, $\overline{\mathcal{A}}$ denote the interior and the closure of a set $\mathcal{A} \subset \mathbb{R}^n$.

2. Setting

Consider plant dynamics of the form

$$\begin{aligned}\dot{x}_\mathrm{p} &= A_\mathrm{p} x_\mathrm{p} + B_\mathrm{p} \mathrm{sat}_{[u^-, u^+]}(u) \\ y &= C_\mathrm{p} x_\mathrm{p} + D_\mathrm{p} \mathrm{sat}_{[u^-, u^+]}(u),\end{aligned} \tag{1}$$

with state $x_\mathrm{p} \in \mathbb{R}^{n_p}$, saturated input $\mathrm{sat}_{[u^-, u^+]}(u) \in [-u^-, u^+] \subset \mathbb{R}^m$ ($u^-, u^+ \in \mathbb{R}^m_{\geq 0}$), output $y \in \mathbb{R}^p$ and matrices A_p, B_p, C_p and D_p of suitable dimensions. Assume that a prescribed linear dynamic output feedback controller be given

$$\begin{aligned}\dot{x}_\mathrm{c} &= A_\mathrm{c} x_\mathrm{c} + B_\mathrm{c} y + v_1 \\ u &= C_\mathrm{c} x_\mathrm{c} + D_\mathrm{c} y + v_2,\end{aligned} \tag{2}$$

such that, with $v_1 = 0$ and $v_2 = 0$, the closed loop (1), (2) is locally exponentially stable. For large responses activating input

saturation, $v = [v_1^\top \ v_2^\top]^\top \in \mathbb{R}^{n_c + m}$ is an input used for anti-windup design aiming at increasing (suitable estimates of) the basin of attraction.

The classical DLAW approach corresponds to selecting

$$\begin{bmatrix}v_1 \\ v_2\end{bmatrix} = \begin{bmatrix}D_{\mathrm{aw},1}(u - \mathrm{sat}_{[u^-, u^+]}(u)) \\ D_{\mathrm{aw},2}(u - \mathrm{sat}_{[u^-, u^+]}(u))\end{bmatrix} \\ = D_\mathrm{aw}(u - \mathrm{sat}_{[u^-, u^+]}(u)), \tag{3}$$

leading to the anti-windup closed loop

$$\begin{aligned}\dot{x} &= A_\mathrm{cl} x + \left(B_{\mathrm{cl},q} + \begin{bmatrix}B_{\mathrm{cl},v_1} & B_{\mathrm{cl},v_2}\end{bmatrix}\begin{bmatrix}D_{\mathrm{aw}_1} \\ D_{\mathrm{aw}_2}\end{bmatrix}\right)\mathrm{dz}_{[u^-, u^+]}(u) \\ u &= C_\mathrm{cl} x + \left(D_{\mathrm{cl},q} + \begin{bmatrix}D_{\mathrm{cl},v_1} & D_{\mathrm{cl},v_2}\end{bmatrix}\begin{bmatrix}D_{\mathrm{aw}_1} \\ D_{\mathrm{aw}_2}\end{bmatrix}\right)\mathrm{dz}_{[u^-, u^+]}(u),\end{aligned} \tag{4}$$

where $x = [x_\mathrm{p}^\top \ x_\mathrm{c}^\top]^\top \in \mathbb{R}^n$, $n = n_p + n_c$, and with the following matrices (see also Zaccarian and Teel (2011, Ch. 4.2 and Ch. 4.2.1)),

$$\left[\begin{array}{c|c|c|c}A_\mathrm{cl} & B_{\mathrm{cl},q} & B_{\mathrm{cl},v_1} & B_{\mathrm{cl},v_2} \\ \hline C_\mathrm{cl} & D_{\mathrm{cl},q} & D_{\mathrm{cl},v_1} & D_{\mathrm{cl},v_2}\end{array}\right] := \tag{5}$$

$$\left[\begin{array}{cc|c|c|c}A_\mathrm{p} + B_\mathrm{p}\Delta_u D_\mathrm{c}C_\mathrm{p} & B_\mathrm{p}\Delta_u C_\mathrm{c} & -B_\mathrm{p}\Delta_u & 0 & B_\mathrm{p}\Delta_u \\ B_\mathrm{c}\Delta_y C_\mathrm{p} & A_\mathrm{c} + B_\mathrm{c}\Delta_y D_\mathrm{p}C_\mathrm{c} & -B_\mathrm{c}\Delta_y D_\mathrm{p} & I & B_\mathrm{c}\Delta_y D_\mathrm{p} \\ \hline \Delta_u D_\mathrm{c}C_\mathrm{p} & \Delta_u C_\mathrm{c} & I - \Delta_u & 0 & \Delta_u\end{array}\right]$$

where we denote $\Delta_u := (I - D_\mathrm{c}D_\mathrm{p})^{-1}$ and $\Delta_y := (I - D_\mathrm{p}D_\mathrm{c})^{-1}$, both of them being invertible under a standard linear well-posedness condition. For the controller (2), we require the following standard assumption.

Assumption 1. The linear closed loop (1), (2) is well-posed, namely matrices Δ_u and Δ_y above are well defined. Matrix A_cl in (4) is Hurwitz. Moreover, $B_\mathrm{p} \neq 0$ and

$$\bar{u} := \tfrac{1}{2}(u^+ + u^-) = \mathbb{1} \in \mathbb{R}^m, \quad u_\circ := \tfrac{1}{2}(u^+ - u^-). \tag{6}$$

define the average saturation range and the average saturation center with an additional constraint. ◇

Linear well-posedness and Hurwitz A_cl are necessary because the anti-windup action must disappear in the small signals regime. Note also that A_cl being Hurwitz implies that the pairs $(A_\mathrm{p}, B_\mathrm{p})$, $(A_\mathrm{c}, B_\mathrm{c})$ are stabilizable. Without the technical assumption $B_\mathrm{p} \neq 0$ the saturation in (1) and the control problem are pointless. The assumption $\bar{u} = \mathbb{1} \in \mathbb{R}^m$ can always be achieved by appropriately scaling the columns of B_p and D_p. To design the anti-windup gain D_aw, let $\alpha > 0$ and $\nu \in (0, 1]$ be fixed, and consider the semi-definite program (SDP)

$$\min_{Q, Y, U, X_1, X_2} \log \det(Q) \quad \text{subject to} \tag{7a}$$

$$Q = Q^\top > 0, \quad U > 0 \text{ diagonal}, \tag{7b}$$

$$\mathrm{He}\begin{bmatrix}A_\mathrm{cl}Q + \alpha Q & B_{\mathrm{cl},q}U + B_{\mathrm{cl},v_1}X_1 + B_{\mathrm{cl},v_2}X_2 \\ C_{\mathrm{cl},u}Q - Y & D_{\mathrm{cl},q}U + D_{\mathrm{cl},v_2}X_2 - \nu U\end{bmatrix} < 0$$

$$\begin{bmatrix}1 & Y_{[k]} \\ Y_{[k]}^\top & Q\end{bmatrix} \geq 0, \quad k = 1, \ldots, n_u. \tag{7c}$$

Based on this SDP, the following proposition is a slight variation of the results in Formentin, Dabbene, Tempo, Zaccarian, and Savaresi (2016, Prop. 4) and Gomes da Silva and Tarbouriech (2005) where we introduce the saturation limits in (9), instead of (7c), so that we allow for the scheduling approach of Section 3. The proposition provides a parametric design procedure for selecting the anti-windup gain D_aw in (3) and to obtain the estimate of the basin of attraction of the origin for the closed loop system (4). The first parameter $\alpha > 0$ allows us to impose a prescribed closed-loop convergence rate, which also provides improved robustness properties with respect to disturbances and noise. The second parameter $\nu \in (0, 1]$ enforces a reduction of

the Lipschitz constant of the explicit solution of the nonlinear algebraic loop in (2) (Grimm, Teel, & Zaccarian, 2003) (Zaccarian & Teel, 2011, §3.4.2), so as to ease its implementation. Increasing α and reducing ν comes at the cost of smaller estimates of the basin of attraction. Including α and ν as optimization variables in (7) would transform the convex SDP in a quasi-convex GEVP, whose solution can be computed via bisection methods.

Proposition 1. *Consider the plant-controller pair* (1), (2), *define* $c = \min([(u^-)^\top \ (u^+)^\top])$ *and select* $\alpha > 0$, $\nu \in (0, 1]$. *Let Assumption 1 be satisfied. Then the SDP* (7) *is feasible for a small enough* $\alpha > 0$ *and a large enough* $\nu \in (0, 1]$. *Moreover, selecting* P *and* D_{aw_1}, D_{aw_2} *as*

$$P = Q^{-1}, \quad D_{\mathrm{aw}_1} = X_1 U^{-1}, \quad D_{\mathrm{aw}_2} = X_2 U^{-1} \tag{8}$$

the algebraic loop in (2) *is well-posed and the set*

$$\{x \in \mathbb{R}^n : |x|_P = \sqrt{x^\top P x} \le c\} \tag{9}$$

is contained in the basin of attraction of the origin for closed loop (4). *Moreover,* $V : \mathbb{R}^n \to \mathbb{R}_{\ge 0}$, $V(x) = x^\top P x$ *is a Lyapunov function satisfying* $\langle \nabla V(x), \dot{x} \rangle \le -2\alpha V(x)$ *for all* $x \in \{x \in \mathbb{R}^n : |x|_P \le c\}$. ⌟

Proof (*SKETCH*)**.** A slight variation of the result can be found in Gomes da Silva and Tarbouriech (2005) or Formentin et al. (2016, Prop. 4). Here, we have included the parameter c in (9) instead of (7c) (i.e., we have switched the roles of c and 1 compared to Formentin et al. (2016) and Gomes da Silva and Tarbouriech (2005)). This is possible due to the homogeneity of the decision variables in (7c) (see Braun et al. (2021, Cor. 2)), which allows rescaling P and all the other decision variables without affecting the choice of D_{aw} in (8). The results in Formentin et al. (2016) and Gomes da Silva and Tarbouriech (2005) only guarantee local exponential stability, but the convergence rate is not specified. The additional parameter $\alpha > 0$ (and the corresponding term αQ in (7b)) guarantees local exponential stability with a prescribed convergence rate i.e., $|x(t)| \le M e^{-\alpha t} |x(0)|$ for all $x(0)$ satisfying (9), and $M > 0$ defined through the eigenvalues of P. The results in Formentin et al. (2016) and Gomes da Silva and Tarbouriech (2005) only cover the case $\nu = 1$. The parameter ν in (7b) introduces a strong well-posedness condition inducing an upper bound on the Lipschitz constant of the solution of the algebraic loop (2), as characterized in Grimm et al. (2003), but does not affect the proof of Formentin et al. (2016, Prop. 4) because negativity of (7b) for some $\nu \in (0, 1]$ implies its negativity with $\nu = 1$. ∎

Remark 1. The nonlinear algebraic loop (4) may be associated with computational issues. When closing the loop (1), (2), (3), it requires solving the nonlinear equation $u = C_c x_c + D_c y + D_{\mathrm{aw}_2} \mathrm{dz}_{[u^-, u^+]}(u)$. This equation can be solved following the techniques in Blanchini, Giordano, Riz, and Zaccarian (2022). Alternatively, when $D_c D_p = 0$ (which can always be ensured by redefining the plant output as $\bar{y} = y - D_p \mathrm{sat}_{[u^-, u^+]}(u) = C_p x_p$), one can impose $D_{\mathrm{aw}_2} = 0$ by removing (setting to zero) variable X_2 in (7). This still allows for D_{aw_1} to be arbitrary and in general leads to effective anti-windup designs. ○

3. Stabilization of a shifted equilibrium

Instead of the origin, we use Proposition 1 to design an anti-windup action focusing on a shifted equilibrium $x_e = (x_{p_e}, x_{c_e})$ of (1) and (2), induced by way of two new correction inputs η_1, η_2 acting as follows

$$\begin{aligned} 0 &= A_p x_{p_e} + B_p u_e, & 0 &= A_c x_{c_e} + B_c y_e + \eta_1, \\ y &= C_p x_{p_e} + D_p u_e, & u_e &= C_c x_{c_e} + D_c y_e + \eta_2. \end{aligned} \tag{10}$$

Input saturation will be accounted for in (10) through the definition in (15). For fixed η, the constraints in (10) can be written as:

$$\underbrace{\begin{bmatrix} A_p & 0 & 0 & B_p & 0 & 0 \\ 0 & A_c & B_c & 0 & I & 0 \\ C_p & 0 & -I & D_p & 0 & 0 \\ 0 & C_c & D_c & -I & 0 & I \end{bmatrix}}_{M :=} \begin{bmatrix} x_{p_e} \\ x_{c_e} \\ y_e \\ u_e \\ \eta_1 \\ \eta_2 \end{bmatrix} = \begin{bmatrix} 0 \\ 0 \\ 0 \\ 0 \end{bmatrix}, \quad M^\perp = \begin{bmatrix} M^\perp_{x_p} \\ M^\perp_{x_c} \\ M^\perp_y \\ M^\perp_u \\ M^\perp_{\eta_1} \\ M^\perp_{\eta_2} \end{bmatrix} \tag{11}$$

where $M^\perp$ generates the kernel of matrix M. In particular, all the equilibria of (10) can be parametrized through a vector $\delta \in \mathbb{R}^\theta$, where $\theta = n_p + n_c + p + m + n_c + m - \mathrm{rank}(M)$ is the dimension of $\mathrm{Ker}(M)$, as follows

$$x_e(\delta) = \begin{bmatrix} x_{p_e}(\delta) \\ x_{c_e}(\delta) \end{bmatrix} = \begin{bmatrix} M^\perp_{x_p} \delta \\ M^\perp_{x_c} \delta \end{bmatrix} = M^\perp_x \delta, \tag{12}$$

$$\eta(\delta) = \begin{bmatrix} \eta_1(\delta) \\ \eta_2(\delta) \end{bmatrix} = \begin{bmatrix} M^\perp_{\eta_1} \delta \\ M^\perp_{\eta_2} \delta \end{bmatrix} = M^\perp_\eta \delta, \tag{13}$$

$$\begin{bmatrix} y_e(\delta) \\ u_e(\delta) \end{bmatrix} = \begin{bmatrix} M^\perp_y \delta \\ M^\perp_u \delta \end{bmatrix}. \tag{14}$$

Remark 2. Since $M \in \mathbb{R}^{(n_p + n_c + p + m) \times (n_p + 2n_c + p + 2m)}$, the parameter θ, representing the dimension of the Kernel of the matrix M, satisfies $\theta \ge n_c + m \ge m \ge 1$. ○

Eqs. (11) are not taking the bounds $u \in [-u^-, u^+]$ into account. To this end we additionally define the set

$$\Delta := \{\delta \in \mathbb{R}^\theta | -u^- \le M^\perp_u \delta \le u^+\} \tag{15}$$

and $\Delta \ne \emptyset$ according to Remark 2 and the assumption that $u^-, u^+ \in \mathbb{R}^m_{>0}$. Using δ, we introduce a generalized anti-windup compensation providing the following selections of the anti-windup compensation signals (v_1, v_2) in (2), to be compared with the classical ones in (3):

$$\begin{aligned} v_1 &= D_{\mathrm{aw},1}(u - \mathrm{sat}_{[u^-, u^+]}(u)) + \eta_1(\delta), \\ v_2 &= D_{\mathrm{aw},2}(u - \mathrm{sat}_{[u^-, u^+]}(u)) + \eta_2(\delta). \end{aligned} \tag{16}$$

With these definitions, the following result about the asymptotic stability of the induced equilibrium $x_{p_e}(\delta)$, $\delta \in \Delta$ in (12) can be stated.

Theorem 1. *Let* $\delta \in \Delta$, *let Assumption 1 be satisfied and fix* $\alpha > 0$ *and* $\nu \in (0, 1]$. *Consider the plant-controller pair* (1), (2), *with the anti-windup compensation* (13), (16). *Define*

$$\beta(\delta) := \min([(u^- + u_e(\delta))^\top \ (u^+ - u_e(\delta))^\top]), \tag{17}$$

and assume that the SDP (7) *is feasible. Select* P *and the static anti-windup gain* D_{aw} *as in* (8). *Then the algebraic loop in* (2), (16) *is well-posed and the set*

$$\mathcal{E}_\delta(P) = \{x \in \mathbb{R}^n : |x - x_e(\delta)|_P \le \beta(\delta)\} \tag{18}$$

is contained in the basin of attraction of the induced equilibrium $x_e(\delta)$ *of the closed-loop system. Moreover,* $V_\delta : \mathbb{R}^n \to \mathbb{R}_{\ge 0}$ *defined as*

$$V_\delta(x) = (x - x_e(\delta))^\top P (x - x_e(\delta)) \tag{19}$$

is a Lyapunov function satisfying $\langle \nabla V_\delta(x), \dot{x} \rangle \le -2\alpha V_\delta(x)$ *for all* $x \in \mathcal{E}_\delta(P)$. ⌟

Remark 3. Based on the definition of η in (13), it holds that $\eta(0) = 0$. Thus, Proposition 1 can be seen as a corollary of Theorem 1.

Here, $\beta : \mathbb{R}^\theta \to \mathbb{R}$ in (17) defines the size of the region for which asymptotic stability of $x_e(\delta)$ is guaranteed. Under Assumption 1, $\beta(\delta) \in [0, 1]$ for all $\delta \in \Delta$, by design. Function β in (18) virtually manipulates the input saturation limits, allowing for larger input margins if $u_e(\delta) = u_\circ$, as defined in (6) (i.e., when stabilizing $x_e(\delta)$) and smaller margins if $|u^- + u_e(\delta)|_1$ or $|u^+ - u_e(\delta)|_1$ are small. This overcomes limitations of Proposition 1 in cases where $|u^+|_1$ or $|u^-|_1$ are small. $\quad\circ$

Proof of Theorem 1. We use Proposition 1 to prove the statement, by appropriately shifting the origin of the plant-controller dynamics (1), (2) as well as the saturation and the deadzone operator. In this context, note that for any $\delta \in \Delta$, the following equalities are satisfied by $u_e(\delta)$ defined in (14),

$$\begin{aligned}
&\mathrm{sat}_{[u^-, u^+]}(u)\\
&\quad = u_e(\delta) + \mathrm{sat}_{[u^- + u_e(\delta), u^+ - u_e(\delta)]}(u - u_e(\delta))
\end{aligned} \tag{20}$$

$$\begin{aligned}
\mathrm{dz}_{[u^-, u^+]}(u) &= u - \mathrm{sat}_{[u^-, u^+]}(u)\\
&= (u - u_e(\delta)) + \mathrm{sat}_{[u^- + u_e(\delta), u^+ - u_e(\delta)]}(u - u_e(\delta))\\
&= \mathrm{dz}_{[u^- + u_e(\delta), u^+ - u_e(\delta)]}(u - u_e(\delta)).
\end{aligned} \tag{21}$$

In the following, let $\delta \in \Delta$ be fixed and let x_{p_e}, x_{c_e}, u_e and y_e denote the corresponding variables defined in (12), (14) where we drop the argument δ for simplicity of notation. Since any plant equilibrium pair (x_{p_e}, u_e) satisfies $0 = A_p x_{p_e} + B_p u_e$ (cf., (11)), with $\delta \in \Delta$ (i.e., $u_e \in [-u^-, u^+]$), we can shift the coordinates as $\tilde{x}_p := x_p - x_{p_e}$, $\tilde{u} := u - u_e$, which leads to the following shifted dynamics, issued from (1), and from replacing the saturation operator with (20):

$$\begin{aligned}
\dot{\tilde{x}}_p = \frac{d}{dt}(x_p - x_{p_e}) &= A_p \tilde{x}_p + B_p(\mathrm{sat}_{[u^-, u^+]}(u) - u_e)\\
&= A_p \tilde{x}_p + B_p \mathrm{sat}_{[u^- + u_e, u^+ - u_e]}(\tilde{u}).
\end{aligned} \tag{22}$$

Similarly, using again (20), the shifted output $\tilde{y} := y - y_e$, with y_e defined in (14), satisfies

$$\begin{aligned}
\tilde{y} = y - y_e &= C_p(x - x_{p_e}) + D_p(\mathrm{sat}_{[u^-, u^+]}(u) - u_e)\\
&= C_p \tilde{x} + D_p \mathrm{sat}_{[u^- + u_e, u^+ - u_e]}(\tilde{u}).
\end{aligned} \tag{23}$$

The conditions (11) and the selection of $\delta \in \Delta$ imply $0 = A_c x_{c_e} + B_c y_e + \eta_1$. Hence, using this condition for the shifted variable $\tilde{x}_c := x_c - x_{c_e}$, together with the controller dynamics (2), the anti-windup action (16), and identity (21), it holds that

$$\begin{aligned}
\dot{\tilde{x}}_c &= A_c x_c + B_c y + v_1 - A_c x_{c_e} - B_c y_e - \eta_1\\
&= A_c \tilde{x}_c + B_c \tilde{y} + v_1 - \eta_1\\
&= A_c \tilde{x}_c + B_c \tilde{y} + D_{\mathrm{aw},1} \mathrm{dz}_{[u^-, u^+]}(u)\\
&= A_c \tilde{x}_c + B_c \tilde{y} + D_{\mathrm{aw},1} \mathrm{dz}_{[u^- + u_e, u^+ - u_e]}(\tilde{u})
\end{aligned} \tag{24}$$

Finally, using the expression of u in (2), of v_2 in (16) and the condition $u_e = C_c x_{c_e} + D_c y_e + \eta_2$ in (11), we obtain the following implicit expression of the shifted controller output, where we use again (21),

$$\begin{aligned}
\tilde{u} := u - u_e &= C_c x_c + D_c y + v_2 - C_c x_{c_e} - D_c y_e - \eta_2\\
&= C_c(x_c - x_{c_e}) + D_c(y - y_e) + D_{\mathrm{aw},2} \mathrm{dz}_{[u^-, u^+]}(u) + \eta_2 - \eta_2\\
&= C_c \tilde{x}_c + D_c \tilde{y} + D_{\mathrm{aw},2} \mathrm{dz}_{[u^- + u_e, u^+ - u_e]}(\tilde{u}).
\end{aligned} \tag{25}$$

Wrapping up, the shifted dynamics (22), (23), (24), (25) correspond to

$$\begin{cases}
\dot{\tilde{x}}_p = A_p \tilde{x}_p + B_p \mathrm{sat}_{[u^- + u_e, u^+ - u_e]}(\tilde{u}),\\[4pt]
\tilde{y} = C_p \tilde{x}_p + D_p \mathrm{sat}_{[u^- + u_e, u^+ - u_e]}(\tilde{u}),\\[4pt]
\dot{\tilde{x}}_c = A_c \tilde{x}_c + B_c \tilde{y} + \tilde{v}_1,\\[4pt]
\tilde{u} = C_c \tilde{x}_c + D_c \tilde{y} + \tilde{v}_2,\\[4pt]
\tilde{v}_1 = D_{\mathrm{aw},1} \mathrm{dz}_{[u^- + u_e, u^+ - u_e]}(\tilde{u}),\\[4pt]
\tilde{v}_2 = D_{\mathrm{aw},2} \mathrm{dz}_{[u^- + u_e, u^+ - u_e]}(\tilde{u}),
\end{cases}$$

which represents the plant-controller pair (1), (2) with the classical anti-windup action (3) for a shifted version $\{u^- + u_e, u^+ - u_e\}$ of the saturation limits. For these shifted limits, Proposition 1 can be applied with $c = \beta(\delta)$, due to the definition in (17). Hence, the convergence results as well as the estimate of the basin of attraction can be concluded from Proposition 1.

Finally, the well-posedness of the algebraic loop in (25) also follows from Proposition 1, since well-posedness of (25) only relies on the properties of $D_{\mathrm{aw},2}$ and the additional signal η is not present. $\quad\blacksquare$

Remark 4. When accounting for the additional signal η injected in the output equation of the controller dynamics (2), through the extended anti-windup action (16), the classical anti-windup closed loop reported in (4) generalizes to the following closed-loop representation of the shifted anti-windup closed loop (1), (2), (16):

$$\begin{aligned}
\dot{x} &= A_{\mathrm{cl}} x + (B_{\mathrm{cl},q} + B_{\mathrm{cl},v} D_{\mathrm{aw}}) \mathrm{dz}_{[u^-, u^+]}(u) + B_{\mathrm{cl},\eta} \eta(\delta)\\
u &= C_{\mathrm{cl}} x + (D_{\mathrm{cl},q} + D_{\mathrm{cl},v} D_{\mathrm{aw}}) \mathrm{dz}_{[u^-, u^+]}(u) + D_{\mathrm{cl},\eta} \eta(\delta)
\end{aligned} \tag{26}$$

where matrices $B_{\mathrm{cl},\eta}$ and $D_{\mathrm{cl},\eta}$ are defined as

$$\left[\frac{B_{\mathrm{cl},\eta}}{D_{\mathrm{cl},\eta}}\right] := \begin{bmatrix} 0 & B_p(I - D_c D_p)^{-1}\\ I & B_c(I - D_p D_c)^{-1} D_p\\ 0 & (I - D_c D_p)^{-1} \end{bmatrix} = \begin{bmatrix} 0 & B_p \Delta_u\\ I & B_c \Delta_y D_p\\ 0 & \Delta_u \end{bmatrix}$$

This representation can be seen as a consequence of the matrices in Zaccarian and Teel (2011, Sections 4.2 and 4.2.1), by considering the additional input η as a specific selection of the disturbance input w characterized in Zaccarian and Teel (2011, Section 4.2). $\quad\circ$

To simplify the notation in the following, we summarize the closed-loop dynamics (26) through

$$\dot{x} = f(x, u(x, \delta), \delta) \tag{27}$$

where the definition of f follows directly from the right-hand side of the first equation in (26) and the definition of $u(x, \delta)$ follows from the second equation in (26).

4. Shifted anti-windup design with increased domain of attraction

In this section we combine Proposition 1 and Theorem 1 to obtain an anti-windup action for the plant-controller pair (1), (2) providing increased estimates of the basin of attraction. To this end, exploiting δ in (26) and (27), given state x we optimize δ to minimize $|x_e(\delta)|$ in (12) such that x is in the ellipsoidal set (18). In this way, while the feedback controller steers x to $x_e(\delta)$, the optimizer continuously shifts $x_e(\delta)$ to the origin. It is proven in our main result that $x_e(\delta)$ reaches the origin in finite time, which additionally implies that $x \to 0$ asymptotically. This intuitive construction is formalized next.

As a first step, note that for a given $\delta \in \Delta$, the value $\beta(\delta)$ in (17) defines the largest level set of the function (19) for which forward invariance of the set $\mathcal{E}_\delta(P)$ defined in (18), and convergence of solutions are guaranteed through Theorem 1. To design a controller with increased guarantees of the basin of attraction relying on Theorem 1, we define the set

$$\mathcal{R} := \bigcup_{\delta \in \mathrm{int}(\Delta)} \mathcal{E}_\delta(P) \tag{28}$$

and the parametric convex optimization problem

$$\begin{aligned}
\delta^\star(x) &:= \underset{\rho \in \Delta}{\mathrm{argmin}} \; \rho^\top H \rho\\
&\text{subject to } |x - x_e(\rho)|_P \le \beta(\rho)
\end{aligned} \tag{29}$$

where H defines the objective function

$$H = (M_x^\perp)^\top M_x^\perp + \mu I \qquad (30)$$

for $\mu \geq 0$. Optimization problem (29) is feasible for all $x \in \overline{\mathcal{R}}$ (i.e., the closure of $\mathcal{R}$) by design according to (18) and the definition of $\mathcal{R}$ in (28). Moreover, $\delta^\star(\cdot) : \text{int}(\mathcal{R}) \to \Delta$ is a Lipschitz continuous function that satisfies $\delta^\star(x) = 0$ for all $x \in \mathcal{E}_0(P)$ (see Braun, Giordano, Kellett, Shames, and Zaccarian (2022, Lemma 1), Braun et al. (2021, Lemma 1) and Hager (1979, Appendix D)).

Remark 5. The objective function (29) minimizes the induced equilibrium in terms of the objective function, i.e., $|x_e(\rho)|^2 + \mu|\rho|^2$ is minimized. The last term $\mu|\rho|^2$ is included to ensure that the objective function is strongly convex. If $(M_x^\perp)^\top M_x^\perp$ is positive definite the term $\mu|\rho|^2$ is not necessary to ensure this property. ∘

Remark 6. The function β defined in (17) is piecewise affine and continuous with at most $2m$ (where $m \in \mathbb{N}$ denotes the dimension of the input u) affine components. Accordingly, optimization problem (29) can be written in form of a standard optimization problem

$$\delta^\star(x) := \arg\min \ \bar{f}(\rho) \qquad (31)$$

subject to $\quad \bar{g}_i(\rho; x) \leq 0, \quad i = 1, \ldots, 2(m + \theta)$

with objective function $\bar{f}(\rho) = \rho^\top H \rho$ and the functions $\bar{g}_i$, $i = 1, \ldots, 2(m + \theta)$, capture the constraints $|x - x_e(\rho)|_P \leq \beta(\rho)$ and $\rho \in \Delta$, respectively. ∘

Based on these definitions we may now introduce the proposed anti-windup scheme as the following state-dependent generalization of (16):

$$\begin{aligned}
v_1 &= D_{\text{aw},1}(u - \text{sat}_{[u^-, u^+]}(u)) + \eta_1(\delta^\star(x)), \\
v_2 &= D_{\text{aw},2}(u - \text{sat}_{[u^-, u^+]}(u)) + \eta_2(\delta^\star(x)), \\
\eta_1(\delta^\star(x)) &= M_{\eta_1}^\perp \delta^\star(x), \quad \eta_2(\delta^\star(x)) = M_{\eta_2}^\perp \delta^\star(x).
\end{aligned} \qquad (32)$$

Here, the expressions of η_1 and η_2 from (13) have been reported for the convenience of the reader. In contrast to (16), the selection of $\delta = \delta^\star(x)$ in (32) is state dependent. The peculiar optimization-based scheduled architecture of our anti-windup compensation scheme (29), (32) is represented in the block diagram of Fig. 1. The anti-windup nature of the scheme in terms of local preservation of the (so-called unconstrained) response induced by controller (2) with $v_1 = 0$, $v_2 = 0$ is a consequence of the fact that $\delta^\star(x) = 0$ for all points $x \in \mathcal{E}_0(P)$. While the deadzone loops highlighted in Fig. 1 resemble typical actions of direct linear anti-windup, the new signal η injected by our scheme provides an important action ensuring that the plant state never exits a certain safe set for large initial conditions. As a consequence, closed-loop modifications are not only enforced when the saturation nonlinearity is activated, but also when the closed-loop state $x = [x_p^\top, x_c^\top]^\top$ belongs to "unsafe" regions where suitable conditioning of the (otherwise linear) closed loop are deemed appropriate. This type of "extended activation" is not new in the literature, as it also appeared in Barbu et al. (2005), Galeani et al. (2007) and Teel (1999) when dealing with exponentially unstable plants and wanting to keep the state within certain inner approximations of the null-controllability region. Our new solution provides an alternative approach whose intuitive effect is well grasped by the architecture shown in Fig. 1. Based on Theorem 1, we may now state the main stability result of this paper, providing a stability guarantee with larger estimates of the basin of attraction.
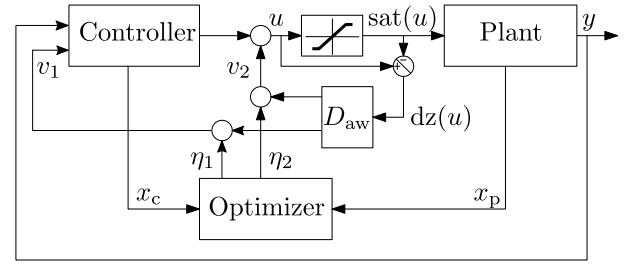

Fig. 1. Block diagram of the proposed optimization-based anti-windup augmentation (29), (32).

Theorem 2. Let Assumption 1 be satisfied, consider $\alpha > 0$, $\nu \in (0, 1]$, $\mu > 0$ and the plant–controller pair (1), (2) with the anti-windup augmentation (32) and P and D_{aw} defined in (8), with $\delta^\star(\cdot)$ denoting the optimizer of (29). Then, the algebraic loop in (2), (32) is well-posed, the solution of (31) is Lipschitz in $\text{int}(\mathcal{R})$, and $\text{int}(\mathcal{R})$ is contained in the basin of attraction of the origin $(x_p, x_c) = 0$ for the closed-loop system (1), (2), (32). ⌟

Proof. The proof follows the same ideas and arguments outlined in Braun et al. (2021, Thm 1). Due to the properties of the optimization problem (29), the function $x \mapsto \delta^\star(x)$ is Lipschitz continuous in $\text{int}(\mathcal{R})$. This follows from the fact that the objective function is strongly convex and the feasible set is convex for all $x \in \text{int}(\mathcal{R})$, Braun et al. (2021, Lemma 1). Combined with the well-posedness of the algebraic loop (established in Proposition 1) this implies that the feedback law u, which is implicitly defined in (2), (32) as $u = C_c x_c + D_c y + D_{\text{aw},2} \, \text{dz}_{[u^-, u^+]}(u) + \eta_2(\delta^\star(x))$, is also Lipschitz.

To prove asymptotic stability, first note that $\delta^\star(x) = 0$ in the neighborhood of the origin (9) denoted by $\mathcal{E}_0(P)$. This fact follows from the definition of the objective function and the definition of the constraints of the optimization problem (29). Accordingly, since the controller (32) coincides with the controller in Proposition 1, asymptotic stability with $\mathcal{E}_0(P)$ as an estimate of the basin of attraction can be concluded.

To complete the proof we need to show that the set $\mathcal{E}_0(P)$ is reached in finite time from any initial state $x \in \text{int}(\mathcal{R})$, from which the assertion about the estimate of the basin of attraction follows. Reaching the set $\mathcal{E}_0(P)$ in finite time is equivalent to $\delta^\star(x(t)) = 0$ for t sufficiently large. According to Theorem 1, for δ constant, the set $\mathcal{E}_\delta(P)$ is forward invariant. Hence, combining the forward invariance with (29) (and in particular with the objective function) implies that $|\delta^\star(x(t))|_H$ is monotonically decreasing. Since $|\cdot|_H \geq 0$ the monotonicity implies that $|\delta^\star(x(t))|_H$ is converging, and convexity of $\delta^\star(x(t)) \in \Delta$ (defined in (15)), monotonicity of $|\delta^\star(x(t))|_H$ and $H > 0$ imply that $\delta^\star(x(t))$ is converging. If $\delta^\star(x(t)) \to \delta^\sharp \neq 0$, then $x(t) \to x_e(\delta^\sharp)$ can be concluded. However, this leads to a contradiction because there exists t such that $x(t) \in \text{int}(\mathcal{E}_{\delta^\sharp}(P))$. Thus $|\delta^\star(x(t))|_H < |\delta^\sharp|_H$. Accordingly, $\delta^\sharp = 0$ and finite time convergence of $\delta^\star(\cdot)$ to 0 can be concluded through the same contradiction argument, completing the proof. ∎

Theorem 2 provides an estimate of the basin of attraction of the closed-loop system (1), (2), (32). Since $\mathcal{R}$ in (28) is defined as the union of infinitely many ellipsoids, an explicit characterization of the set is unfortunately not possible. Nevertheless, it is straightforward to verify if a state satisfies $x \in \mathcal{R}$ by checking if (29) is feasible for $x \in \mathbb{R}^n$. Moreover, an inner approximation of $\mathcal{R}$ can be easily obtained by taking the union of $\mathcal{E}_{\delta_i}(P)$ for a finite number of points $\delta_i \in \text{int}(\Delta)$, $i \in \{1, \ldots, N\}$, $N \in \mathbb{N}$.

Remark 7. Due to the Lipschitz properties established in Theorem 2, the closed-loop system is regular enough for asymptotic stability to be robust in the small as characterized in Goebel, Sanfelice, and Teel (2012, Ch. 7). This robustness implies graceful degradation of the nominal closed-loop properties, under the action of disturbances, noisy measurements from low-cost sensors, sampled-data and even PWM implementations (Teel & Nesic, 2010) of the feedback law, as well as approximate solutions of the optimization problem (31), as long as disturbances and noise are sufficiently small. Robustness in the large and a rigorous study of the impact of large disturbances and noise on the closed-loop dynamics will be studied in future work. ○

5. Controller implementation

We discuss here three efficient controller implementation solutions, which help running our feedback on the low-cost Arduino-based experimental device discussed in Section 6: (a) the algebraic loop in (2), (32) needs to be solved in real time, (b) the optimization problem (29) needs to be solved in real time. With respect to (a), in the single input case, i.e., $m = 1$, an explicit solution of the algebraic loop is given by $u = y_c + D_{\mathrm{aw},2}(I - D_{\mathrm{aw},2})^{-1} \mathrm{dz}_{[-u^-, u^+]}(y_c)$, with $y_c := C_c x_c + D_c y + \eta(\delta^\star)$ (see Blanchini et al. (2022, Eq. (11))). This expression emerges from representing the second expression in (2) and (32) as $u = y_c + D_{\mathrm{aw},2} \mathrm{dz}_{[u^-,u^+]}(u)$. For the multi-input setting, efficient ways to solve the algebraic loop are discussed in Blanchini et al. (2022), for example. Moreover, the algebraic loop can be often avoided through the condition in Remark 1 if the implementation of the algebraic loop is an issue.

About (b), since (29) is a convex optimization problem, it can be solved efficiently through standard convex optimization algorithms. Moreover, under additional assumptions on δ or the function $\beta(\cdot)$ defined in (17), optimization (29) can be further simplified. Here, two simplified cases are discussed. However, it is worth noting that instead of updating δ in continuous time, it is also possible to update δ at discrete time steps in a sample-and-hold fashion, if solving (29) in real time is an issue. This implementation can be done without loss in terms of the size of the estimate of the basin of attraction in Theorem 1, and details can be found in Braun et al. (2022, Section IV).

5.1. Explicit computation of $\delta^\star \in \mathbb{R}$

In the case that δ is one dimensional, a (semi) explicit solution of (29) can be derived. The derivation follows, with minimal adaptations, from the result derived in Braun et al. (2021, Theorem 2) and the properties in Braun et al. (2021, Lemma 1). In particular, according to Braun et al. (2021, Lemma 1) the optimal solution $\delta^\star(x)$ in (29) satisfies $\delta^\star(x) = 0$ if $|x|_P \leq \beta(0)$ and $|x - M_x^\perp \delta^\star(x)|_P = \beta(\delta^\star(x))$ otherwise, where we have used the notation in (12). Under the additional observation that for $\dim(\delta) = 1$ and $\dim(u) = 1$, the function $\beta(\cdot)$ satisfies

$$\beta(\delta) = \begin{cases} u^- + M_u^\perp \delta, & \text{if} M_u^\perp \delta \in [-u^-, u_\circ] \\ u^+ - M_u^\perp \delta, & \text{if} M_u^\perp \delta \in [u_\circ, u^+]. \end{cases} \tag{33}$$

Therefore, whenever $\delta^\star(x) \neq 0$, one of the following two quadratic equations must hold for $\delta^\star$ (we drop the argument of $\delta^\star(x)$ to simplify the notation)

$$\begin{aligned} |x - M_x^\perp \delta^\star|_P^2 &= (u^- + M_u^\perp \delta^\star)^\top (u^- + M_u^\perp \delta^\star), \\ |x - M_x^\perp \delta^\star|_P^2 &= (u^+ - M_u^\perp \delta^\star)^\top (u^+ - M_u^\perp \delta^\star). \end{aligned} \tag{34}$$

Since $\beta(\cdot)$ is concave, and according to the objective function in (29), the smallest value $\delta H \delta$ satisfying $M_u^\perp \delta \in [-u^-, u^+]$ and one of Eqs. (34) consequently defines the optimal solution $\delta^\star$. Introducing

$$\begin{aligned} a &= (M_x^\perp)^\top P M_x^\perp - (M_u^\perp)^\top M_u^\perp, \\ b^\pm &= -2x^\top P M_x^\perp \pm 2(u^\pm)^\top M_u^\perp, \\ c^\pm &= x^\top P x - (u^\pm)^\top u^\pm, \end{aligned}$$

the solutions of the quadratic equations are given by

$$\delta_{1,2} = \frac{-b^- \pm \sqrt{(b^-)^2 - 4ac^-}}{2a}, \quad \delta_{3,4} = \frac{-b^+ \pm \sqrt{(b^+)^2 - 4ac^+}}{2a},$$

in the case where $a \neq 0$. In the case where $a = 0$, the four candidates reduce to the two possible solutions $\delta_5 = -\frac{c^-}{b^-}$, $\delta_6 = -\frac{c^+}{b^+}$. This result is summarized in the following proposition.

Proposition 2. *Consider* (29) *and assume that* $\dim(\delta) = 1$ *and* $\dim(u) = 1$. *Then for all* $x \in \mathcal{E}_0(P)$ *it holds that* $\delta^\star(x) = 0$. *Moreover, for* $x \in \mathcal{R} \backslash \mathcal{E}_0(P)$ *it holds that*

$$\begin{aligned} \delta^\star(x) &\in \{\delta_1, \delta_2, \delta_3, \delta_4\} \text{ if } (M_x^\perp)^\top P M_x^\perp \neq (M_u^\perp)^\top M_u^\perp, \\ \delta^\star(x) &\in \{\delta_5, \delta_6\} \qquad \text{if } (M_x^\perp)^\top P M_x^\perp = (M_u^\perp)^\top M_u^\perp. \end{aligned}$$

While this result is limited to the case $\dim(\delta) = 1$, it can be used to obtain a suboptimal solution of (29) in the multi-dimensional setting $\dim(\delta) > 1$ under the assumption that a feasible point $\delta^\# \in \Delta$, $|x - \delta^\#|_P \leq \beta(\delta^\#)$ is known. In particular, the solution of

$$\begin{aligned} \kappa^\star &:= \underset{\kappa \in \mathbb{R}}{\arg\min} \; \kappa^2 \\ &\text{subject to } |x - \kappa \cdot x_e(\rho^\#)|_P \leq \beta(\kappa \cdot \rho^\#) \end{aligned} \tag{35}$$

can be used to define $\kappa^\star \delta^\#$ as a suboptimal solution of (29) with the property $(\kappa^\star \delta^\#)^\top H(\delta^\# \kappa^\star) \leq (\delta^\#)^T H \delta^\#$. Since κ is one dimensional in (35), a similar reasoning as in Proposition 2 can be used for computing the optimizer $\kappa^\star$. The suboptimal solution $\kappa^\star \delta^\#$ can be used as an initial guess for (29), i.e., to warmstart an appropriate convex optimization algorithm. Note that depending on $\dim(u)$, the function β in (33) is the minimum over multiple affine functions, leading to additional equality constraints in (34).

5.2. A constant β-function

Another simplification of (29) arises when function $\beta(\cdot)$ defined in (17) is constant, i.e., $M_u^\perp$ defined in (14) satisfies $M_u^\perp = 0$. This assumption is satisfied in the application discussed in Section 6, for example. In this case, we can define the parameter

$$\bar{\beta} = \beta(\delta) = \min([(u^-)^\top (u^+)^\top]), \tag{36}$$

and optimization problem (29) becomes

$$\begin{aligned} \delta^\star(x) &:= \underset{\rho \in \Delta}{\arg\min} \; \rho^\top H \rho \\ &\text{subject to } \left| P^{\frac{1}{2}} x - P^{\frac{1}{2}} M_x^\perp \rho \right|^2 \leq \bar{\beta}^2. \end{aligned} \tag{37}$$

Most importantly, the $2m$ inequality constraints in (29), also discussed in Remark 6, reduce to a single inequality constraint, independent of the dimensions of u and δ.

Following the presentation in Beck (2014, Chapter 11.4), for fixed $x \in \mathrm{int}(\mathcal{R})$, the Lagrangian $\mathcal{L} : \Delta \times \mathbb{R}_{\geq 0} \to \mathbb{R}$ of (37) can be defined as

$$\mathcal{L}(\rho, \lambda) = \rho^\top H \rho + \lambda \left(\left| P^{\frac{1}{2}} x - P^{\frac{1}{2}} M_x^\perp \rho \right|^2 - \bar{\beta}^2 \right)$$

and the KKT conditions are given by

$$H\rho + \lambda\left((M_x^\perp)^\top P M_x^\perp \rho - (M_x^\perp)^\top P x\right) = 0, \tag{38}$$

$$\lambda\left(\left|P^{\frac{1}{2}}x - P^{\frac{1}{2}}M_x^\perp \rho\right|^2 - \bar\beta^2\right) = 0, \tag{39}$$

$$\lambda \geq 0, \qquad \left|P^{\frac{1}{2}}x - P^{\frac{1}{2}}M_x^\perp \rho\right|^2 \leq \bar\beta^2. \tag{40}$$

Note that the constraint $\rho \in \Delta$ is never active for $x \in \text{int}(\mathcal{R})$, according to the properties established in Braun et al. (2022, Lemma 1) and Braun et al. (2021, Lemma 1). By (40), we have either that $\lambda^\star = 0$ or $\lambda^\star > 0$. If $\lambda^\star = 0$, then (38) implies $\delta^\star(x) = 0$. If $\lambda^\star > 0$, then (38) implies

$$\delta^\star(x) = \left(H + \lambda^\star (M_x^\perp)^\top P M_x^\perp\right)^{-1} \lambda^\star (M_x^\perp)^\top P x \tag{41}$$

and $\lambda^\star$ is defined as the solution of $\phi(\lambda^\star) = 0$, where $\phi(\cdot)$ is defined as

$$\phi(\lambda) = \left|x - M_x^\perp\left(H + \lambda(M_x^\perp)^\top P M_x^\perp\right)^{-1} \lambda(M_x^\perp)^\top P x\right|_P^2 - \bar\beta^2.$$

This expression is obtained by substituting $\rho = \delta^\star(x)$ from (41) in (39) divided by $\lambda^\star > 0$. A solution of $\phi(\lambda) = 0$ can for example be obtained efficiently through a bisection method (Beck, 2014, Chapter 11.4). In particular, for $x \in \text{int}(\mathcal{R}) \backslash \mathcal{E}_0(P)$, it holds that $\phi(0) = |x|_P^2 - \bar\beta^2 > 0$, $\phi(\lambda^\star) = 0$ and $\phi(\lambda) < 0$ for all $\lambda > \lambda^\star$.

6. Experimental validation

In this section, we illustrate the performance of the controller on the low-cost, segway-like vehicle developed in Brentari, Zambotti, Zaccarian, Bosetti, and Biral (2015). The open-loop plant has an eigenvalue at the origin (comprising the arbitrary position variable) and our anti-windup solution, as emphasized in the introduction, manages to obtain an unbounded basin of attraction: any arbitrarily large rest-to-rest maneuver can be obtained with our scheme. We illustrate that DLAW alone cannot obtain this. Alternative examples, whose shifted equilibria require nonzero inputs u_e may be issued, e.g., from the longitudinal aircraft dynamics in Barbu et al. (2005), to also illustrate the desirable features of our solution in handling asymmetric saturation limits. The corresponding results are not included here due to lack of space.

6.1. Segway dynamics

Following Brentari et al. (2015), let $J = j_1 j_2 - (m_b lr \cos(\vartheta))^2$, the segway dynamics are described through

$$\ddot{s} = \frac{j_1 \dot\vartheta^2 - m_b gl\cos(\vartheta)}{J} m_b lr^2 \sin(\vartheta) - v_f \dot s + \frac{j_1 + m_b lr\cos(\vartheta)}{J}\tau r$$

$$\ddot\vartheta = \frac{gj_2 - m_b lr^2\cos(\vartheta)\dot\vartheta^2}{J} m_b l\sin(\vartheta) - \frac{j_2 + m_b lr\cos(\vartheta)}{J}\tau$$

$$\dot\tau = -\frac{R_r}{L_r}\tau + \frac{2K_\tau}{L_r}(\hat u - K_e \dot s).$$

Here, s denotes the position, ϑ denotes the angle of the inverted pendulum in terms of the deviation from the upright position, τ denotes the torque exerted at the wheels, and $\hat u$ is the voltage applied to the motors. The term $K_e \dot s$ is the back electromotive force (EMF), and $j_1 = j_b + m_b l^2$ and $j_2 = j_w + (m_b + m_w)r^2$ combine the body and wheels inertia. A description of the other parameters can be found in Table 1. According to Table 1, the torque dynamics is more than one order of magnitude faster than the mechanical one. Moreover, the back EMF component $K_e \dot s$ is identified and compensated as in Brentari et al. (2015). Therefore, we replace the dynamics of τ with the static mapping $\tau = K_u \hat u$, where K_u is again reported in Table 1. The input voltage is limited to the symmetric interval $\hat u \in [-V_{\max}, V_{\max}]$ or, equivalently, to $u \in [-1, 1]$, by considering the coordinate

Table 1
Segway parameters.

Variable	Value	Meaning
m_w	0.850 kg	Mass of the wheels
m_b	3.358 kg	Mass of the body
j_w	0.0036 kg m^2	Inertia of the wheels
j_b	0.748 kg m^2	Inertia of the body
g	9.81 m/s^2	Gravitational acceleration
r	0.086 m	Wheel radius
v_f	0.1 s^{-1}	Viscous friction coefficient
l	0.274 m	Distance of CoG from the wheel spin axis
R_r	2.15 Ω	Motor winding resistance
L_r	0.0008 H	Motor winding inductance
K_τ	0.6808 N m/A	Current to torque constant
K_u	0.15 N m/V	Voltage to torque constant
$V_{\max}$	4 V	Maximal (minimal) input voltage

transformation $u = \frac{1}{V_{\max}}\hat u$ in terms of a dimensionless input u. Note that the coordinate transformation is necessary to ensure that Assumption 1 in terms of the average saturation range is satisfied. To obtain a linear system of the form (1) we consider the plant state $x_p = [s \quad \vartheta \quad \dot s \quad \dot\vartheta]^\top$.

Linearizing the nonlinear dynamics about the origin, leads to the matrices

$$A_p = \begin{bmatrix} 0 & 0 & 1 & 0 \\ 0 & 0 & 0 & 1 \\ 0 & \frac{-g(m_b lr)^2}{j_1 j_2 - (m_b lr)^2} & -v_f & 0 \\ 0 & \frac{gj_2 m_b l}{j_1 j_2 - (m_b lr)^2} & 0 & 0 \end{bmatrix}, \quad B_p = \begin{bmatrix} 0 \\ 0 \\ rK_u\frac{j_1 + m_b lr}{j_1 j_2 - (m_b lr)^2} \\ -K_u\frac{j_2 + m_b lr}{j_1 j_2 - (m_b lr)^2} \end{bmatrix}$$

defining the first equation in (1). To obtain the second equation in (1), we define $y = x_p$, i.e., $C_p = I$ denotes the identity matrix and $D_p = 0$. Note that the linearization is independent of the position s. Accordingly, the distance to the origin does not have an impact on the modeling error introduced through the linearization.

6.2. LMI-based controller synthesis

To stabilize the origin for the segway, we consider a PID controller in the variables s and ϑ, defined as

$$u = k_1 s + k_2 \vartheta + k_3 \dot s + k_4 \dot\vartheta + k_5 \int s + k_6 \int \vartheta$$

with controller gains $k_\ell \in \mathbb{R}$, $\ell \in \{1, \ldots, 6\}$, to be defined. Through the definition $x_c = k_5 \int s + k_6 \int \vartheta$, i.e., $\dot x_c = k_5 s + k_6 \vartheta$, the dynamic controller

$$\dot x_c = A_c x_c + B_c x_p, \qquad u = C_c x_c + D_c x_p$$

with $A_c = 0$, $B_c = [k_5, k_6, 0, 0]$, $C_c = 1$, and $D_c = [k_1, k_2, k_3, k_4]$, is obtained.

Inspired by the approach in Cunico, Cenedese, Zaccarian, and Borgo (2022), we exploit an LMI-based technique to tune the controller gains k_ℓ, $\ell \in \{1, \ldots, 6\}$. Through the definitions

$$A_o = \begin{bmatrix} A_p & 0 \\ B_c & 0 \end{bmatrix}, B_o = \begin{bmatrix} B_p \\ 0 \end{bmatrix}, K = \begin{bmatrix} D_c & k_0 \end{bmatrix}, z = \begin{bmatrix} x_p \\ x_c \end{bmatrix}, \tag{42}$$

we can write the linear plant-controller closed loop with the PID controller as a state feedback

$$\dot z = A_{cl}z = (A_o + B_o K)z = \begin{bmatrix} A_p + B_p D_c & B_p k_0 \\ B_c & 0 \end{bmatrix} z$$

where A_{cl} is defined in 5. Fixing the integral gains k_5 and k_6, we can tune the feedback gains $K = [D_c k_0]$ to guarantee stability of the linear closed loop, while shaping the transient response. To this end, we define a sector of the complex plane using three parameters:

- $\bar\alpha \geq 0$ defines the maximum allowed spectral abscissa,

- $\sigma > \bar{\alpha}$ defines the maximum magnitude of the closed-loop eigenvalues,
- $\vartheta \in [0, \pi/2]$ defines the width of a sector characterizing a guaranteed damping factor.

Then, the feedback gains $\{k_0, \ldots, k_4\}$ that constrain the closed-loop eigenvalues in the prescribed sector (see Cunico et al. (2022, Fig. 10)) are obtained by solving the following optimization problem:

$$\min_{\substack{W \in \mathbb{R}^{5 \times 5}, \\ X \in \mathbb{R}^{1 \times 5}, \; \gamma \in \mathbb{R}}} \gamma \quad \text{subject to}$$

$$W = W^\top > I, \quad M + M^\top + 2\bar{\alpha} W < 0, \tag{43a}$$

$$\begin{bmatrix} (M + M^\top)\sin(\vartheta) & (M - M^\top)\cos(\vartheta) \\ (M^\top - M)\cos(\vartheta) & (M + M^\top)\sin(\vartheta) \end{bmatrix} \leq 0, \tag{43b}$$

$$\begin{bmatrix} \sigma W & M^\top \\ M & \sigma W \end{bmatrix} \geq 0, \quad \begin{bmatrix} \gamma I & X^\top \\ X & \gamma I \end{bmatrix} \geq 0. \tag{43c}$$

Here, $M := A_o W + B_o X \in \mathbb{R}^{5 \times 5}$, $X \in \mathbb{R}^{1 \times 5}$ is associated to the control gains via $K = X W^{-1}$, $W \in \mathbb{R}^{5 \times 5}$ is a Lyapunov certificate, and $\gamma > 0$ is used to limit the norm of the control gains. The left constraint in (43a) imposes $\|K\| \leq \|X\| \|W^{-1}\| \leq \|X\|$, while the right constraint in (43c) ensures, via a Schur complement, that $\|X\| \leq \gamma$. The right constraint in (43a), the left constraint in (43b) and (43c) limit the eigenvalues of the closed-loop matrix to the sector defined by $\bar{\alpha}$, ϑ, and σ. Problem (43) is feasible if the pair (A_o, B_o) is controllable (Cunico et al., 2022, Proposition 3). Therefore, selecting $K = X W^{-1}$ guarantees that:

- the closed-loop matrix $A_{\text{cl}} = A_o + B_o K$ has eigenvalues λ_i, $i = 0, \ldots, 4$ with $|\lambda_i| \leq \sigma$,
- the damping factor of the poles is larger than $\cos(\vartheta)$,
- $\text{Re}(\lambda_i) < -\bar{\alpha}$ for all $i = 0, \ldots, 4$ (i.e., A_{cl} is Hurwitz).

These properties can be verified following the same arguments outlined in Cunico et al. (2022, Proposition 3).

6.3. Simulations and experiments

Using the parameters in Table 1 together with the gains $k_5 = 1$ and $k_6 = 10$, the open loop matrices

$$A_p = \begin{bmatrix} 0 & 0 & 1 & 0 \\ 0 & 0 & 0 & 1 \\ 0 & -2.16 & -0.1 & 0 \\ 0 & 11.01 & 0 & 0 \end{bmatrix}, \quad B_p = \begin{bmatrix} 0 \\ 0 \\ 0.39 \\ -0.48 \end{bmatrix},$$

as well as the controller matrix B_c are obtained. Based on these definitions, it is straightforward to verify that the pair (A_o, B_o) in (42) is controllable. Moreover, for $\bar{\alpha} = 0.5$, $\sigma = 10$ and $\vartheta = \frac{\pi}{30}$ LMI (43) leads to the controller gain $K = [25.43, 193.47, 29.29, 57.50, 5.82]$, which ensures that the eigenvalues of A_{cl} satisfy the properties defined through $\bar{\alpha}$, σ and ϑ, as discussed in Section 6.2. With the selection above for the controller gain K, we proceed with the definition of the anti-windup design. Matrix $M^\perp$ defined in (11) is given by

$$M_{x_p}^\perp = M_y^\perp = \begin{bmatrix} -0.04 & -0.03 \\ 0 & 0 \\ 0 & 0 \\ 0 & 0 \end{bmatrix}, M_u^\perp = [0 \; 0],$$

$$M_{x_c}^\perp = [0.95 \; -0.20], \quad M_\eta^\perp = \begin{bmatrix} 0.25 & 0.17 \\ 0.15 & 0.96 \end{bmatrix}.$$

Accordingly, δ is two-dimensional and the function β is constant (since $M_u^\perp = 0$) and satisfies $\bar{\beta} = \beta(\delta) = 1$ for all $\delta \in \Delta$, thus allowing us to use the approach in Section 5.2. To obtain the antiwindup gain D_{aw}, we solve the SDP (7) for $\alpha = 0.05$ and $\nu = 0.999$ and obtain the antiwindup gain D_{aw} as well as the positive definite matrix P:

$$D_{\text{aw}} = \begin{bmatrix} -2.18 \\ 0.60 \end{bmatrix}, \; P = \begin{bmatrix} 100.9 & 574.9 & 114.7 & 169.8 & 3.9 \\ 574.9 & 4192.5 & 695.7 & 1254.8 & 22.1 \\ 114.7 & 695.7 & 135.7 & 207.1 & 4.4 \\ 169.8 & 1254.8 & 207.1 & 376.1 & 6.5 \\ 3.9 & 22.1 & 4.4 & 6.5 & 0.17 \end{bmatrix}.$$
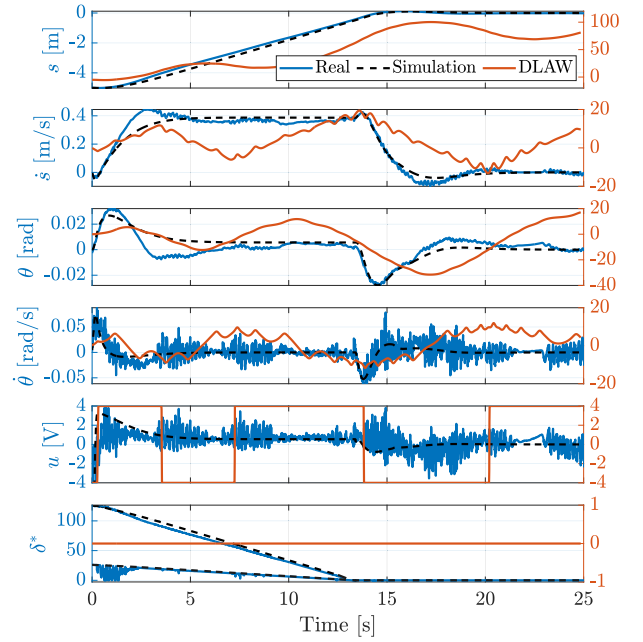

Fig. 2. Closed-loop solution $x = [x_p^\top, x_c]^\top$, input u, and optimal δ obtained for the segway initialized at $x_0 = [-5 \; 0 \; 0 \; 0 \; 0]^\top$, with (blue, experimental) and without (orange, simulation) equilibrium shifting. (For interpretation of the references to color in this figure legend, the reader is referred to the web version of this article.)

Fig. 2 shows both simulation and experimental results of the overall controller driving the state $x(t)$ with initial condition $x_0 = [-5 \; 0 \; 0 \; 0 \; 0]^\top$ to the origin,[1] and a comparison with DLAW (the simulation in orange, which is equivalent to our controller with $\eta = 0$). From this comparison, it is clear that shifting the equilibrium is key to ensuring convergence to the origin. The black and orange simulation results in Fig. 2 are a lot smoother than the measurements obtained from the experiment (shown in blue). This is due to the sensor noise, and to the dithering-like sinusoidal signal injected at the voltage input to compensate for the mechanical backlash (see the discussion in Brentari et al. (2015)). Since the input u is a voltage reference implemented as a PWM signal, we emphasize that this noisy behavior has little or no effect on the smoothness of the mechanical motion. By solving the optimization problem (29), we may check that the initial condition satisfies $x_0 \in \mathcal{R}$. Due to the structure of $M_u^\perp$ it holds that $\Delta = \mathbb{R}^2$. This fact, together with the property that $\beta(\delta) = 1$ for all $\delta \in \Delta$, and the definition of $M_x^\perp$ implies that

$$\mathcal{R} = \mathcal{E}_0(P) \oplus \text{span} \left\{ \begin{bmatrix} 1 \\ 0 \\ 0 \\ 0 \\ 0 \end{bmatrix}, \begin{bmatrix} 0 \\ 0 \\ 0 \\ 0 \\ 1 \end{bmatrix} \right\},$$

where $\oplus$ represents the Minkowski sum. Accordingly, for this particular example, a rather simple representation of $\mathcal{R}$ is obtained. For (29), the parameter μ is selected as $\mu = 0$ (which is valid selection since $(M_x^\perp)^\top M_x^\perp$ is positive definite) and (29) is solved approximately using the method discussed in Section 5.2. Due to the robustness discussed in Remark 7, we may implement our feedback in a low-cost Arduino board, which runs at 100 Hz and where 8 bisection steps are performed at every time step for the computation of $\delta^\star(x)$. Despite the low-cost nature of our device, as shown in Fig. 2, the real dynamics well matches the simulated one and the segway successfully converges the origin.

---

[1] A video of the experiment can be found at the address: https://youtu.be/Sm3niDz4Jmw.

7. Conclusions

We addressed an anti-windup problem, providing a novel scheme extending the classical direct linear static anti-windup paradigm by way of a recent technique proposed in the context of bounded stabilization, consisting in suitably scheduling a shifted equilibrium point. For this anti-windup setting, we showed that the resulting scheme shares commonalities with existing advanced anti-windup solutions specifically focusing on an inner approximation of the null-controllability region. Rigorous results prove the effectiveness of our approach and experimental tests on a segway-like vehicle confirmed the desirable anti-windup compensation action. While our approach enjoys some intrinsic robustness properties due to the fact that the controller is provably Lipschitz continuous, a rigorous analysis of the robustness properties as well as the effect of an observer in the closed-loop system are still missing.

References

Barbu, C., Galeani, S., Teel, A. R., & Zaccarian, L. (2005). Robust antiwindup for manual flight control of an unstable aircraft. *International Journal of Control*, 78(14), 1111–1129.

Beck, A. (2014). *Introduction to nonlinear optimization: theory, algorithms, and applications with MATLAB*. SIAM.

Blanchini, F., Giordano, G., Riz, F., & Zaccarian, L. (2022). Solving nonlinear algebraic loops arising in input-saturated feedbacks. *IEEE Transactions on Automatic Control*.

Braun, P., Giordano, G., Kellett, C. M., Shames, I., & Zaccarian, L. (2022). Optimizing shifted stabilizers with asymmetric input saturation. Accepted for publication in IEEE Transactions on Automatic Control, Preprint: https://hal.science/hal-03586545/.

Braun, P., Giordano, G., Kellett, C. M., & Zaccarian, L. (2021). An asymmetric stabilizer based on scheduling shifted coordinates for single-input linear systems with asymmetric saturation. *IEEE Control Systems Letters*, 6, 746–751.

Brentari, M., Zambotti, A., Zaccarian, L., Bosetti, P., & Biral, F. (2015). Position and speed control of a low-cost two-wheeled, self-balancing inverted pendulum vehicle. In *IEEE int. conference on mechatronics* (pp. 347–352).

Cao, Y. Y., Lin, Z., & Ward, D. G. (2002). An antiwindup approach to enlarging domain of attraction for linear systems subject to actuator saturation. *IEEE Transactions on Automatic Control*, 47(1), 140–145.

Cunico, D., Cenedese, A., Zaccarian, L., & Borgo, Mauro M. (2022). Nonlinear modeling and feedback control of boom barrier automation. *IEEE/ASME Transactions on Mechatronics*.

Dai, D., Hu, T., Teel, A. R., & Zaccarian, L. (2009). Piecewise-quadratic Lyapunov functions for systems with deadzones or saturations. *Systems & Control Letters*, 58(5), 365–371.

Formentin, S., Dabbene, F., Tempo, R., Zaccarian, L., & Savaresi, S. M. (2016). Robust linear static anti-windup with probabilistic certificates. *IEEE Transactions on Automatic Control*, 62(4), 1575–1589.

Galeani, S., Teel, A. R., & Zaccarian, L. (2007). Constructive nonlinear anti-windup design for exponentially unstable linear plants. *Systems & Control Letters*, 56(5), 357–365.

Goebel, R., Sanfelice, R. G., & Teel, A. R. (2012). *Hybrid dynamical systems: modeling, stability, and robustness*. Princeton University Press.

Grimm, G., Teel, A. R., & Zaccarian, L. (2003). Establishing Lipschitz properties of multivariable algebraic loops with incremental sector nonlinearities. In *IEEE conference on decision and control*.

Hager, W. W. (1979). Lipschitz continuity for constrained processes. *SIAM Journal on Control and Optimization*, 17(3), 321–338.

Hu, T., Teel, A. R., & Zaccarian, L. (2008). Anti-windup synthesis for linear control systems with input saturation: achieving regional, nonlinear performance. *Automatica*, 44(2), 512–519.

Lu, L., & Lin, Z. (2011). Design of a nonlinear anti-windup gain by using a composite quadratic Lyapunov function. *IEEE Transactions on Automatic Control*, 56(12), 2997–3001.

Mariano, S., Blanchini, F., Formentin, S., & Zaccarian, L. (2020). Asymmetric state feedback for linear plants with asymmetric input saturation. *IEEE Control Systems Letters*, 4(3), 608–613.

Mulder, E. F., Kothare, M. V., & Morari, M. (2001). Multivariable anti-windup controller synthesis using linear matrix inequalities. *Automatica*, 37(9), 1407–1416.

Nicotra, M. M., & Garone, E. (2018). The explicit reference governor: A general framework for the closed-form control of constrained nonlinear systems. *IEEE Control Systems Magazine*, 38(4), 89–107.

Queinnec, I., Tarbouriech, S., Valmorbida, G., & Zaccarian, L. (2022). Design of saturating state feedback with sign-indefinite quadratic forms. *IEEE Transactions on Automatic Control*, 67(7), 3507–3520.

Rawlings, J. B., Mayne, D. Q., & Diehl, M. (2017). *Vol. 2, Model predictive control: theory, computation, and design*. Nob Hill Publishing.

Gomes da Silva, J. M., Jr., & Tarbouriech, S. (2005). Anti-windup design with guaranteed regions of stability: an LMI-based approach. *IEEE Transactions on Automatic Control*, 50(1), 106–111.

Sontag, E. D. (1984). An algebraic approach to bounded controllability of linear systems. *International Journal of Control*, 39(1), 181–188.

Tarbouriech, S., & Turner, M. (2009). Anti-windup design: an overview of some recent advances and open problems. *IET Control Theory & Applications*, 3(1), 1–19.

Teel, A. R. (1999). Anti-windup for exponentially unstable linear systems. *International Journal of Robust and Nonlinear Control*, 9, 701–716.

Teel, A. R., & Nesic, D. (2010). Averaging for a class of hybrid systems. *Dynamics of Continuous, Discrete and Impulsive Systems*, 17(6), 829–851.

Zaccarian, L., & Teel, A. R. (2011). *Modern anti-windup synthesis: control augmentation for actuator saturation*. Princeton (NJ): Princeton University Press.

Philipp Braun received the Diploma in mathematics from Technical University Kaiserslautern in 2012, and the Ph.D. degree in mathematics from the University of Bayreuth in 2016. He is currently a Senior Lecturer in the School of Engineering at the Australian National University, Canberra.

Abhishek Bhardwaj received his Ph.D. in 2020 from the Mathematical Sciences Institute at the Australian National University (ANU). He held post-doc positions in the MAC team at LAAS-CNRS (2020–2021) and in the School of Engineering at the ANU (2021–2023). Currently he is a post-doc fellow in the Mathematical Sciences Institute at the ANU.

Mirko Brentari received a Ph.D. in automatic control from the University of Trento, with focus on hybrid controls for mechatronic systems. In 2018–2019 he was a post-doc scholar at Politecnico di Milano working on control of automotive systems, such as active suspensions and electric drivelines. In 2019, he moved to the industry, working on control and software in Dana Inc. up to 2023, and then in JLR Ltd.

Luca Zaccarian has been an Assistant Professor and then an Associate Professor with the University of Roma Tor Vergata, Rome, Italy, since 2000. In 2011, he was the Directeur de Recherche at the Laboratoire d'Analyse et d'Architecture de Systems-CNRS, Toulouse, France. Since 2013, he is also a part-time Professor with the University of Trento, Italy.

Matteo Saveriano is an assistant professor with the University of Trento, Italy. Previously, he was an assistant professor at the University of Innsbruck and a post-doctoral researcher at the German Aerospace Center (DLR). He is an Associate Editor for RA-L and IJRR, and the coordinator of the EU Horizon project INVERSE.